Design of Experience to Evaluate the Interfacial Compatibility on High Tenacity Viscose Fibers Reinforced Polyamide-6 Composites

Baptiste P. Revol, Madeline Vauthier, Matthieu Thomassey, Michel Bouquey, Frédéric Ruch, Michel Nardin

Design of Experience to Evaluate the Interfacial Compatibility on High Tenacity Viscose Fibers Reinforced Polyamide-6 Composites

Baptiste Paul Revol,[1,2,3*] Madeline Vauthier,[2,3,4] Matthieu Thomassey,[1] Michel Bouquey,[3,4] Frédéric Ruch,[1] Michel Nardin[2]

[1] Pôle Ingénierie des Polymères et Composites, Cetim Grand Est, F-68200 Mulhouse, France

[2] Université de Haute-Alsace, CNRS, IS2M UMR 7361, F-68100 Mulhouse, France

[3] Université de Strasbourg, F-67081 Strasbourg, France

[4] Université de Strasbourg, CNRS, Institut Charles Sadron UPR 22, F-67000 Strasbourg, France

*to whom correspondence should be addressed. E-mail : baptiste.revol@gmail.com

Abstract

In recent years, natural fibers reinforced composites have received much attention because of their lightweight, recyclable, nontoxic, low cost and biodegradable properties. However, compatibility between hydrophilic natural fiber and hydrophobic polymer is low. One way to increase the fiber/matrix compatibility is to treat the fiber surface, using hydroxyl groups present on the upper layer of the high tenacity viscose. However, hydroxyl groups are not always accessible on the fibers surface due to impurities. It is thus mandatory to study the various possibilities to determine a good cleaning treatment, which furthermore does not have a negative influence on the mechanical properties of the fibers. In this article, (3-aminopropyl)triethoxysilane (APTES) is used to functionalize the fiber surface after cleaning them, in order to prepare the fibers for reactive injection of polyamide-6. In order to determine the influence of each cleaning/treatment on the physical and chemical properties of the fibers and to determine optimal treatments to increase fibers/matrix compatibility, various characterization methods (XPS, FTIR-ATR, SEM, EDX) were combined to theoretical results obtained by a design of experience.

Keywords: A. Natural fiber composites; B. Fiber/matrix compatibilization; B. Surface treatments; C. Design of experience; E. Plasma treatment

1. Introduction

Currently, composites using a thermosetting polymer matrix are mainly used compared to thermoplastic ones.[1,2] However, thermosetting polymers are hardly recyclable and may require

the use of pollutant solvents. For environmental reasons and to have good mechanical properties, we decided to use thermoplastic polymer (polyamide-6) matrix reinforced by high tenacity viscose (HTV) fibers.[3–6] Indeed, Pickering *et al*. described the recent interest for natural fiber composites due to their low environmental impact (renewable source, little energy), low cost and their wide range of applications (for instance door panels, railcars, engine, sun visors, seat backs or exterior panels)[3] but, none of the presented studies used HTV fibers as reinforcement. For example, while polyamide-6 was used with cellulose reinforcement[7,8] or with natural fibers (pineapple leaf fibers)[9] it was never used with continuous HTV fibers implemented by reactive injection. Experimentally, fibers are wetted with a reactive mixture composed of ε-caprolactame, an initiator (sodium caprolactamate) and an activator (N,N-hexane-1,6-diylbis(hexahy-dro-2-oxo-1H-azepine-1-carboxamide)). This technique has two major advantages: (i) experimental conditions are very close to real composite reactive transfer molding (RTM)[10,11] and (ii) the cellulosic fibers are not degraded during preparation. When optimized, the high tenacity viscose/polyamide-6 system could find applications in the automobile sector,[12] with the production of recyclable composites presenting high mechanical properties. Moreover, it is well known that the fiber/matrix interface compatibility plays a crucial role in the transfer of mechanical properties from the polymer matrix to the fiber.[13,14] It is then mandatory to investigate and improve this compatibility. In this purpose and in order to limit the influence of the cellulosic surface on the polymerization, fibers' cleaning and functionalization are fundamental steps.[15–18] Indeed, the surface of cellulosic fibers can be naturally (triglycerides, waxes, hemicellulose, pectin, proteins or minerals) or artificially (sizing agents and oils used during the implementation) contaminated.[19] As a first step, the most common cleaning treatments (alkaline solution,[13,20] surfactant in a basic medium,[19] hot ethanol solution[21,22] and argon or oxygen plasma treatment[23–25]) are tested on the HTV fibers. Once the most effective cleaning treatment has been selected, it is applied in combination with a functionalization with (3-aminopropyl)triethoxysilane.[26–28] It is then necessary to determine parameters for verifying the effectiveness of the treatment of viscose. For instance, the probability of failure modeled according to a 2-parameter Weibull equation[29,30] was determined to ensure that treatments did not degrade the mechanical properties of the fibers. Finally, a design of experience is carried out to study the interactions between the surface properties (chemical and physical one) after cleaning and/or functionalization steps and the conversion rate of PA6 polymerization. The design of

experience brings new information about the fibers/matrix interactions taking place during the preparation of HTV/PA6 composites.

2. Materials & methods

2.1. Materials

Non-treated high tenacity viscose fibers “Viscord Bohemia Super 2” were supplied by TextilCord (Luxembourg) in the form of a yarn of 2440 dtex containing 1320 filaments in the bundle. The density of viscose was 1.5 10^3 kg/m^3 and the theoretical fiber diameter was equal to 12.5 µm (value calculated from the data given by the supplier).

Concerning the polymeric resin of polyamide-6 (PA6), the reactive mixture consisted of three components: (i) a monomer, ε-caprolactam (CL) named AP-Nylon® Caprolactam solid (99%, Mw = 113.16 g/mol), (ii) an initiator, Brüggolen C10 (sodium caprolactamate, 1 mol/kg concentration in caprolactam) and (iii) an activator, Brüggolen C20P (N,N-hexane-1,6-diylbis(hexahy-dro-2-oxo-1H-azepine-1-carboxamide), 2 mol/kg concentration in caprolactam). CL, C10 and C20P were supplied in sealed polyethylene-lined aluminum drums (Brüggemann Chemical, Germany). After opening, sealed boxes were properly closed and stored in freezing bags filled with dry argon atmosphere.

Pluronic® F-127 (Sigma), a triblock copolymer of hydrophobic polypropylene glycol framed by two hydrophilic blocks of polyethylene glycol (PEG-PPG-PEG), was used as a non-ionic surfactant. The silane compound, (3-aminopropyl)triethoxysilane (APTES), was supplied by Sigma. All products were used as received without further processing or purification.

2.2. Methods

Surface cleaning and functionalization of high tenacity viscose (HTV) fabrics were carried out using a design of experience to determine the different interactions that can occur. The treatment conditions were summed up in Table 1 after selecting four factors: the plasma power, the plasma treatment time, the APTES amino-silane concentration and the APTES treatment time.

2.2.1. Liquid phase cleaning

Sodium solution (NaOH) treatments were carried out in beakers at room temperature for 30 minutes, with 1 g of fiber per 20 mL of solution. The concentration of NaOH was equal to 0.5w%

or 8w%. Pluronic® F-127 concentration was equal to 0.1w%. It was combined with sodium carbonate (0.1w%) for the treatment to take place in basic medium.
Ethanol treatments (EtOH) were carried out at 50°C for 30 minutes or under Soxhlet for 6 hours.

2.2.2. Plasma treatment

Plasma treatments were carried out in a closed plasma-assisted chemical vapor deposition (PACVD) reactor from PLASSYS (MDS 100, pressure down to 2 x 10^{-7} mbar). The reactor was equipped with a gas inlet and outlet. For the preliminary cleaning tests, plasma treatments on HTV fabrics were carried out for 5 minutes at a fixed power (50 W) at a constant pressure (1 mbar) in a closed chamber, saturated with argon or oxygen gas. Then, for the design of experience, plasma treatments were performed in the same chamber, with a power ranging from 10 to 60 W for a given time.

2.2.3. Surface functionalization

Functionalization treatments with (3-aminopropyl)triethoxysilane (APTES) were carried out after plasma cleaning, in ethanol/water (80/20) medium for a given time and with a given APTES concentration. Treatments were carried out at room temperature on fabric surfaces approximately equal to 5x7 cm^2. After treatment, fabrics were put in an oven at 120°C for 2 hours and then cleaned with ethanol for 30 minutes under gentle stirring.

All characterization techniques are described in Supporting Information (1. Experimental section).

3. Results and discussion

3.1. Cleaning treatments

High tenacity viscose (HTV) was tested in two forms: in the form of filaments, and in the form of fabrics. Preliminary cleaning tests were carried out on HTV filaments.
Some of the most common cleaning methods described in the literature (alkaline solution,[13,20] surfactant in a basic medium,[19] hot ethanol solution[21,22] and argon or oxygen plasma treatment[23–25]) were first tested on the filaments to determine the treatment of greatest interest for possible industrial applications.

3.1.1. Liquid phase cleaning of filaments

Liquid phase cleanings were carried out with NaOH, sodium carbonate or ethanol solutions. NaOH (concentration equal to 0.5w% or 8w%) and sodium carbonate (concentration equal to 0.1w%) treatments occurred at room temperature, while ethanol cleaning was carried out at 50°C. X-ray photoelectron spectroscopy was known to be an effective way to check the surface condition before and after cleaning steps.[22,31] It was important to point out that impurities (zinc, sulfur, nitrogen) were present in small amounts on the surface because of the cellulose treatments. Some traces of silicon and sodium were sometimes observed. However, these contaminations did not influence the results discussed (Table 2). The O/C ratio gave an indication of the amount of hydroxyl groups available on the surface. The amount of **C**-C groups gave a direct indication of the amount of impurities present at the surface because the theoretical cellulose did not have any. Finally, **C**OOR groups were of interest when the functionalization of the surface was taken into consideration.

NaOH treatments were commonly used (mercerization) and can effectively clean the surface in many cases. [13,20] However, its influence was not significant here. Indeed, the amount of **C**-C groups did not change between uncleaned viscose and after 8w% NaOH treatment, and decreased from 15% to 12% in the case of treatment at 0.5w% NaOH. However, the O/C ratio varied from 53 to 60% for both sodium hydroxide concentrations. A decrease in free -OH groups after treatment with sodium hydroxide was sometimes observed.[32] Since the surface treated with sodium hydroxide was swollen and reactive,[33] it may react with impurities at the end of the treatment.

Sodium carbonate (Na_2CO_3) treatments were often used for basic cleaning in combination with a polar or an apolar surfactant.[19,34] In this study, the combination of Pluronic® F-127 (an apolar surfactant) with Na_2CO_3 gave interesting results since the O/C ratio increased from 53% to 61% without changing the amount of **C**-C groups. So, a larger proportion of the **C**OOR groups for this cleaning may correspond to **C**-O-H groups but impurities remained present on the surface.

More interesting results were obtained by extraction in ethanol. Indeed, the O/C ratio approached the expected theoretical ratio (from 53% to 68%) and the amount of **C**-C groups decreased to 5%. These results were consistent with those of Rjiba *et al.* for cotton cleaning by extraction under Soxhlet in ethanol.[21]

Despite interesting results obtained with liquid phase treatments by extraction in ethanol, this treatment lacked industrial adaptability (mandatory heating, impurities brought to the surface, use

of organic solvent, fibers swelling, etc.). In this purpose, further research was conducted by studying the efficiency of a plasma treatment.

3.1.2. Plasma treatment to efficiently clean high tenacity viscose filaments

Plasma technology offers many interesting possibilities for the production of high value-added materials. Here, plasma treatments with argon or oxygen gas were carried out for 5 minutes (power = 50 W) before analyzing the fibers by XPS. These results were compared to reference, untreated fibers (Table 3). Argon plasma treatment should have theoretically cleaned the surface without functionalizing it. However, the O/C ratio increased significantly (from 53 to 70%) after this treatment. This was also the case for the amount of **C**-C groups (from 14.7% to 17%) and **C**OOR groups (from 0.7% to 8.2%). **C**OOR groups corresponded to functionalization of the surface and **C**-C groups usually came from the presence of surface impurities. So, argon plasma treatment cleaned the surface while degrading it (**C**-C groups formed by chain breaks). Since the reactive, cleaned surfaces were exposed to air for a short time before XPS analysis, the surfaces may have partially been functionalized by the oxygen of the air. This method (functionalizing polymers through exposure to atmosphere after argon plasma treatment) had actually been used by Short's team.[35]

In the case of oxygen plasma, O/C ratio was equal to 83%, (similar to that of the theoretical cellulose). The surface was not degraded (amount of **C**-C groups equal to 2.4%) and functionalized (**C**OOR groups present at 8.2%). Indeed, unlike argon plasma, oxygen plasma was known to lead to a combined effect of cleaning and functionalization.[24,36]

For both types of plasma, a functionalization of the surface was observed. However, this was probably not caused by the same mechanism. In the case of argon treatment, the surface was cleaned and reactive after treatment, but also degraded. Subsequently, this surface reacted with the oxygen present in the air. In the case of treatment with oxygen plasma, the surface was better cleaned and not degraded (decrease in the amount of **C**-C groups), but also functionalized by reactions with oxygen during the plasma treatment. Similar observations and conclusions were made by Hua *et al.* when comparing oxygen and argon treatments on a cellulosic surface.[37]

So, oxygen plasma was an interesting choice to clean (and partially functionalize) cellulosic surfaces. It was however important to note that the effect of plasma treatment on the physical and chemical properties of the surface strongly depended on the process parameters.[23,38,39]

3.1.3. High tenacity viscose fabrics cleaning with various processes

The previous parts showed interesting results concerning plasma cleaning for HTV filaments. It was also mandatory to verify these results for a fabric, having more surface impurities. In Table 4, plasma treatment was proved to be effective for cleaning the fabrics' surface, despite a surface initially having a large amount of impurities. Indeed, O/C ratios were lower than in the case of the filaments, cleaning was at least as effective since this ratio increased by 118% between an untreated and a 5-minute treated sample. Moreover, the effectiveness of the treatment was dependent on the treatment time. Indeed, the O/C ratio was constant for a 5-minute treatment (O/C = 70% for 10 W and 60 W). The proportions of the different groups were similar in both cases. So, a maximum level of cleaning was achieved under these two conditions.

A 10 W, 1 min plasma treatment was carried out and the amount of **C**-C groups did not change and remained about 48% but the O/C ratio increased from 32% to 36%, proving that this cleaning was not effective. Moreover, a 60 W, 1 min plasma treatment ended up with an O/C ratio increase up to 52% and a decreasing amount of **C**-C groups down to 36%, suggesting that the cleaning of the surface began but was not complete. The amount of **C**OOR groups however reached a value of approximately 10%, equal to that reached after 5-minute treatments.

These observations suggested that, in these conditions, plasma processing was power- and time-dependent until a maximum level of cleaning was reached beyond which process time has no influence. For a higher power and/or a longer processing time, we guessed that the surface may have been degraded by the plasma treatment.[40–42] This solventless, vapor phase treatment seemed more interesting for industrial applications than liquid phase cleaning. However, it was mandatory to determine whether such a treatment had an influence on the mechanical properties of the HTV, and to what extent the surface quality influenced the functionalization mechanisms.

3.2. Oxygen plasma cleaning

In this part, the effect of oxygen plasma treatment was verified by comparing the properties of untreated HTV filament (CNRT) and oxygen plasma treated filament extracted from bundles at 50 W for 5 minutes (CRO2).

3.2.1. Mechanical properties

The diameter of the monofilaments was first measured from a longitudinal observation of the monofilaments (Figure 1) and no significant difference was observed whether the filament was cleaned with 50 W, 5 min oxygen plasma (13.9 ± 1 µm) or not (13.4 ± 1 µm). So, the same diameter value was used for mechanical properties calculus in both cases to allow the comparison of the mechanical properties. Indeed, in order to ensure that plasma treatment did not degrade the mechanical properties of the fibers, they had been tensile tested and compared with untreated fibers (Figure 2). In Figure 2.a, for an untreated filament (CRNT), the average value of rupture stress was 586 ± 64 MPa while it was equal to 636 ± 76 MPa for the plasma treated filament. As a first approximation, there was no significant difference in the rupture stress between these two samples. The Weibull modulus[30] was then estimated to be 10 for the treated filament, compared with a nearly similar value of 11 for the untreated one, which meant that the distribution of defects in the monofilaments was almost identical. In Figure 2.b, the probability of failure modeled according to a 2-parameter Weibull equation was represented and proved that the O_2-plasma treatment had no influence on the rupture stress. Finally, mechanical tests also revealed no significant difference of Young's modulus and elongation at break between treated and untreated filaments (Figure 3). Indeed, Young's moduli were respectively equal to 12 ± 2 GPa and 15 ± 3 GPa for treated and untreated viscose filaments and elongation at break was equal to 12 ± 3% for the treated filament and 13 ± 2% for the untreated one.

In conclusion, oxygen plasma treatment did not modify the mechanical properties of the HTV fabrics, proving that the treatment did not degrade the fabrics. However, the influence on surface properties was clearly spotted by XPS analyzes. Although plasma treatment was effective, it was difficult to deeply analyze its influence. This was one of the reasons why cleaning and surface treatment were simultaneously investigated for further analysis.

3.3. Cleaning and treatment of high tenacity viscose filaments

The objective here was to treat a surface cleaned by oxygen plasma with (3-aminopropyl)triethoxysilane (APTES). However, plasma treatment conditions must be optimized to allow the best cleaning. In addition, whatever the plasma treatment used, the properties of the cleaned surface evolved in contact with air. It was therefore decided to analyze the synergy of cleaning and treatment by functionalizing the surface just after cleaning. In this way, by optimizing

the conditions of cleaning and functionalization, the influence of air on the reactive surface was limited.

A design of experience (Table SI1) approach allowed us to determine the interactions between the different factors (cleaning and functionalization parameters). Thus, it was theoretically possible to quantify the effect of plasma cleaning on the functionalization treatment.

3.3.1. Determination of silane amount and polymerization conversion rate

Before considering the implementation of the design of experience, it was necessary to define a quantity to quantify the effectiveness of cleaning. This was why the amount of nitrogen on the surface of the samples was investigated by Fourier transform infrared spectrometry (FTIR-ATR) on the treated fabrics. Indeed, this parameter indicated the total amount of amino-silane APTES grafted and/or condensed on the surface of the sample. Moreover, the degree of conversion of polyamide-6 after wetting the treated fibers in the reaction mixture, an interesting parameter to verify that the treatment had no negative influence on the polymerization, was previously studied and published by our group.[4]

3.3.1.1. Infrared spectroscopy

By infrared spectroscopy (FTIR-ATR), we observed a variation in peak intensity (absorbance) depending on the treatment conditions. In Figure 4, the peak at 1560 cm^{-1} on the treated fibers corresponded to the $-NH_2$ groups present on the surface of the samples.[30,43] This peak was absent for the untreated HTV, so it allowed to determine the total amount of APTES present on the surface, including the grafted or not grafted amino-silane in hydrolyzed or condensed form. The FTIR curves were normalized with the peak at 1640 cm^{-1} which correspond to adsorbed water. The correlation between the peak corresponding to the $-NH_2$ groups and the amount of silane at the surface was verified in the following section. A not shown peak at 1740 cm^{-1} only for the untreated fabric corresponded to C=O bonds[26] due to impurities. In some cases, a peak at 1480 cm^{-1} was observed, it could correspond to $-NH_3^+$ groups formed by protonation of $-NH_2$ groups during exposure to air.[44]

Other peaks could have been interesting to observe, especially the Si-OH groups (3030-3630 cm^{-1} [30]) to determine the amount of hydrolyzed silane, or Si-O-C (1104 cm^{-1}). However, the characteristic peaks of the HTV were very intense in these areas (-OH 3380 cm^{-1}, COC and CO

between 1159 and 1000 cm^{-1}), it is therefore difficult to analyze silane peaks at these wavenumbers.

3.3.1.2. X-ray Photoelectron Spectroscopy (XPS)

Analyzing XPS spectra allowed the determination of the amount of nitrogen present on the surface. Since the untreated fabric did not possess (or in negligible quantity) nitrogen groups, it was assumed that the nitrogen amount visible by XPS analysis is totally due to the presence of silane (grafted, condensed or not grafted and uncondensed hydrolyzed) on the surface of the fabric. An XPS analysis was performed on four processed samples to verify the correlation between the amount of nitrogen quantified by XPS and the peak intensity of the $-NH_2$ groups observed by FTIR-ATR at 1560 cm^{-1} (Figure 5). The analysis of the intensity of the peak at 1560 cm^{-1} by FTIR-ATR was therefore an effective means of evaluating the amount of nitrogen present on the surface of the HTV.

3.3.2. Design of experience

The first step was to define the factors of interest for the study as well as the experimental field explored. Factors identified as having an influence on the results were: plasma power, plasma treatment time, APTES concentration and APTES treatment time (Table 1). The treated samples always had the same surface of 5x7 cm^2. The levels of plasma power and plasma time factors were selected after preliminary experiments on cotton and high tenacity viscose (HTV). The APTES concentration parameters and APTES treatment time were determined from the literature.[26,45] Once the factors and their levels of variation had been determined, it was possible to draw up an design of experience (Table SI3).

The conversion rate of polyamide-6 determined by ^{1}H-NMR (Y_2) varied from 57% to 72%, except in one case. It was interesting to note that the influence of the treatment conditions on the conversion rate was relatively limited, except in the case of experiment 13 (Y_2 = 16%) (Table SI3). In this particular case, the tissue was poorly cleaned (10 W, 1 min) and the treatment was carried out at high concentration for a long time (5w%, 2 h). Maybe APTES was present in excessive amounts on the surface of the sample in grafted and condensed form, but also in hydrolyzed form which would then disrupt the polymerization.

In the studied experimental domain, the four best conversion rates were obtained for experiments number 6, 10, 11 and 16 (low amount of APTES) with values of 69, 69, 72 and 72% respectively. The conversion rate after wetting a reference sample of untreated HTV by the reactive mixture (and polymerization) was 61%. The plasma/APTES treatment therefore allowed a slight improvement in the polymerization of the reaction mixture. From an experimental point of view, it would then be possible to choose one of these conditions to allow the fabrication of composites whose polymerization would theoretically not be disturbed.

The normalized infrared intensity (*i.e.*, the amount of nitrogen at the surface of the samples) varied from 0.5 to 4 a.u. However, at this stage of the analysis, it was impossible to conclude on the optimum amount of APTES to add. Indeed, a greater amount of silane on the surface of the HTV did not necessarily imply a better fiber/matrix interface. For example, the largest amount of APTES corresponded to the lowest conversion rate (experiment 13). So, it probably existed a maximum amount of silane beyond which the polymerization was disturbed.

In order to deepen the analysis, the interactions between the factors were investigated in order to determine which parameters had the greatest influence on the responses studied (namely the amount of nitrogen groups and the conversion rate).

3.3.3. Coefficients study: amount of silane on the treated fibers

Incertitude on the coefficients was evaluated in order to only consider the significative coefficients (Table 5). The study of the coefficients was first carried out on the amount of nitrogen present on the surface, determined by infrared spectroscopy. The details of the coefficient calculations were explained in Supporting Information.

The significant coefficients for the amount of silane on the fibers are presented in Figure 6. For example, when the concentration of (3-aminopropyl)triethoxysilane (coefficient C) increased from 0.5w% to 5w%, the amount of nitrogen present at the surface of the sample increased by an average of 0.43*2 = 0.86 (around 60%). With the same analyze, we noted that two single interactions (C and D) and two multiple interactions (ABD and ABCD) had a positive effect on the amount of nitrogen at the surface. The only interaction having a negative impact was the one combining plasma time, APTES concentration and APTES time (BCD).

3.3.3.1. Single interactions

The design of experience proved that the APTES concentration (C) had a positive effect on the amount of silane on the surface (Figure 6). In 2002, Gandini's team demonstrated that the adsorption of APTES-type silanes on the surface of cellulose was dependent on the initial concentration[26] and, according to the work of Brochier-Salon *et al.*, the percentage of hydrolyzed silane was constant during a fixed time.[28] So, it was consistent to observe an effect of the APTES concentration independently of the other parameters because APTES could react with a -OH group of the cellulosic surface and with a -OH group available on a silane molecule already grafted on the surface.

When APTES treatment time (D) rised from 30 mins to 2 hrs, the amount of APTES on the surface increased for around 0.86 a.u., *i.e.* around 60%. The dependence of the amount of silane present at the surface as a function of time had also been observed for the functionalization of porous silicone surfaces by Aissaoui *et al* and by Majoul *et al.* They reached a plateau value after respectively 12 hours[46] and 24 hours[47]. This increase was attributed to the adsorption of APTES by the surface to an upper limit and the grafting mechanisms were represented by a model of nucleation and growth on a heterogeneous surface.

3.3.3.2. Multiple interactions

Although interactions ranked higher than two were difficult to interpret from a physical point of view, it was intriguing to note that plasma processing parameters (A and B) had an influence as multiple interactions (ABD, BCD and ABCD) but were not significative as a double interaction. These interactions were still interesting to determine that the silane grafting was influenced by the surface cleaning and to verify that the cleaning of the surface depended on the plasma conditions.

3.3.4. Coefficients study: polyamide-6 conversion rate

Incertitude on the coefficient was evaluated in order to only consider the significative coefficients (Table 5). As presented in Figure 7, almost all factors were significant for the study of the conversion rate.

3.3.4.1. Single interactions

Interestingly, plasma treatment time (D) had an influence on the amount of silane but none on the conversion rate. Since better cleaning previously resulted in a better conversion rate, it was normal

to observe that plasma power (A) and plasma treatment time (B) had a positive influence on the conversion rate (Figure 7).

However, increasing APTES concentration (C) had a negative effect on the conversion rate while it had a positive effect on the amount of silane at the surface (Figure 6). This observation was consistent with the experiment 13 previously discussed (Table SI3) for which the high amount of silane at the surface (4 a.u.) was accompanied by a low conversion rate (16%). So, it was necessary to graft a sufficient quantity of APTES to improve the fiber/matrix interface, but low enough not to disturb the polymerization reaction.

3.3.4.2. Multiple interactions

By comparing Figure 6 and Figure 7, it was interesting to observe that double interactions (AB, AC, AD, BD, CD) had an influence on the PA6 conversion rate but not on the amount of silane at the surface. First, the AB interaction had a negative influence on the conversion rate whereas plasma power (A) and plasma treatment time (B) had a positive influence when considered individually. Thus, a combination of high power/high time lead to a degradation of the surface [48,49] and/or the creation of new functional groups (Table 4), disrupting the polymerization reaction. Then, correlations between one cleaning-parameter (A or B) and one functionalization-parameter (C or D) demonstrated that the combined effect of cleaning and functionalization had a positive effect on the conversion rate (see AC, AD and BD interactions). Finally, CD interaction (APTES concentration and APTES treatment time) negatively affected the PA6 conversion rate, confirming that too much silane on the surface interfered with the PA6 polymerization.

Concerning triple interactions, we interestingly observed that ABD interaction had a negative effect on the conversion rate (Figure 7) but a positive one on the amount of silane (Figure 6) while BCD interaction had a positive effect on the conversion rate (Figure 7) but a negative one on the amount of silane (Figure 6).

As a conclusion from all the above mentioned studies, we hypothesized about silane grafting mechanisms in the presented case: the hydrolyzed silane was grafted onto the surface-available -OH groups, possibly according to a Langmuir model.[26] In parallel, it condensed both in the solution and on the surface (eventually according to a nucleation and growth model[50]). This

approach was consistent with the mechanisms reported in Schwartz's review on the formation of monolayers.[51]

It would be interesting to further correlate the amount of silane condensed on the surface with the amount of APTES present in solution and the conversion rate.

3.4. Complementary characterizations

For model surfaces such as silicon wafers, the high-resolution X-ray photoelectron spectroscopy (XPS) spectrums were useful to observe the Si-O-Si groups resulting from condensation or grafting of silanes. However, for HTV, this distinction was not possible. So, XPS wide spectrum analysis was performed on the four most interesting samples selected using the design of experience (Table 6). These results corresponded to those used to plot the correlation between the amount of nitrogen observed by XPS and by FTIR-ATR (Figure 5).

For treated samples, the presence of silane on the surface as a function of the amount of nitrogen and silicon groups was identified. As silicon was a relatively common contaminant, the amount of silane was assumed to be equal to the amount of nitrogen present at the surface of the samples. As indicated in Table 6, the amount of silane on the surface thus varied between 4.5% and 11% depending on the treatment carried out. Moreover, it was proved in the literature that a correlation existed between the amount of nitrogen present at the surface and the thickness of the layer formed on silicon wafers.[52] So, a quantity of nitrogen equal to 2% would then correspond to a layer of about 10 Å and a layer of about 50 Å for 4.5% of nitrogen. Curiously, percentages of nitrogen and silicon on the samples' surface were rarely equivalent although they were similar, maybe due to impurities present on the HTV.

Scanning electronic microscopy (SEM) analyses were also used to investigate the surface covering of three functionalized samples. The analysis was completed by an Energy Dispersive X-ray spectroscopy (EDX) to know the local chemical composition of the surface. The results are presented in Supporting Information (Figure SI1, Figure SI2).

As a conclusion, complementary analyzes carried out after surfaces-functionalization to complete FTIR-ATR analyzes, confirmed the presence of silane groups on the surface of treated samples.

The amount of silane at the surface was dependent on the treatment conditions and was not homogeneously distributed over the entire treated surface.

4. Conclusion

The study of various cleaning treatments allowed identifying an efficient and non-polluting cleaning treatment: oxygen plasma cleaning. However, the reactivity of the surface after treatment led to subsequent reactions with the air. So, a combined study of cleaning and functionalization was an interesting alternative.

Investigating the amount of silane on the fibers/fabrics surface was a useful parameter to validate the interest of the cleaning and to be aware of the interactions involved in silane grafting. After proving that the amount of silane present on the surface could easily be determined by FTIR-ATR spectra, the conversion rate was an interesting tool to verify that the polymerization was not disturbed. The complex study of interactions showed that a large amount of silane at the surface was not necessarily beneficial to the conversion rate. Indeed, a study of surface treatments with a design of experience was complex because many parameters needed to be considered. Such an approach nevertheless provided answers to implementation issues regardless of the complexity of the mechanisms that occurred. This study by design of experience revealed at least 3 treatment conditions to allow the fabrication of composites. It was also possible to control the amount of grafted silane on high tenacity viscose fibers in order to compatibilize them with a polymer (polyamide-6) matrix.

Finally, the examination of these treatments on polyamide-6 / high tenacity viscose composites properties will provide answers to processing questions in view of their use in industry. Since the fabrication of the composite materials related to this paper would induce a lot of additional experiments and results, it deserves a standalone study.

Acknowledgements

The authors thank Philippe Fioux, Philippe Kunemann and Aissam Airoudj for their help with surface characterizations and access to the IS2M characterization platforms. Dr. B.P. Revol thanks gratefully Cetim Grand Est for the machines access and fundings.

References

[1] T. Johnson, Thermoplastic vs. Thermoset Resins, ThoughtCo. 27 (2020)

[2] A.B. Strong, Fundamentals of Composites Manufacturing: Materials, Methods, and Applications, Society of Manufacturing Engineers (2008), 164. ISBN 13: 9780872638549

[3] K.L. Pickering, M.G.A. Efendy, T.M. Le, A review of recent developments in natural fibre composites and their mechanical performance, Compos. Part Appl. Sci. Manuf. 83 (2016) 98–112. https://doi.org/10.1016/j.compositesa.2015.08.038.

[4] B.P. Revol, M. Thomassey, F. Ruch, M. Bouquey, M. Nardin, Single fibre model composite: Interfacial shear strength measurements between reactive polyamide-6 and cellulosic or glass fibres by microdroplet pullout test, Compos. Sci. Technol. 148 (2017) 9–19. https://doi.org/10.1016/j.compscitech.2017.05.018.

[5] C.V. Nikonovich, N.G. Kerimova, N.D. Burchanova, K.U. Usmanov, The supermolecular structure of viscose fibers and its dependence on spinning conditions, J. Polym. Sci. Polym. Symp. 42 (1973) 1625–1637. https://doi.org/10.1002/polc.5070420365.

[6] L. Caramaro, Fibres et Fils à Usage Technique, Ed. Techniques Ingénieur. am5118 (2005). https://www.techniques-ingenieur.fr/base-documentaire/materiaux-th11/materiaux-composites-presentation-et-renforts-42142210/fibres-et-fils-a-usage-technique-am5118

[7] F.C. Fernandes, R. Gadioli, E. Yassitepe, M.A. De Paoli, Polyamide-6 composites reinforced with cellulose fibers and fabricated by extrusion: Effect of fiber bleaching on mechanical properties and stability, Polymer Composites, 38 (2015). https://doi.org/10.1002/pc.23587

[8] Y. Peng, D.J. Gardner, Y. Han, Characterization of mechanical and morphological properties of cellulose reinforced polyamide 6 composites, Cellulose, 22 (2015) 3199–3215. https://doi.org/10.1007/s10570-015-0723-y

[9] K. Panyasart, N. Chaiyut, T. Amornsakchai, O. Santawitee, Effect of Surface Treatment on the Properties of Pineapple Leaf Fibers Reinforced Polyamide 6 Composites, Energy Procedia. 56 (2014) 406-413. https://doi.org/10.1016/j.egypro.2014.07.173

[10] K. van Rijswijk, H.E.N. Bersee, Reactive processing of textile fiber-reinforced thermoplastic composites – An overview, Compos. Part Appl. Sci. Manuf. 38 (2007) 666–681. https://doi.org/10.1016/j.compositesa.2006.05.007.

[11] M. Thomassey, B. Paul Revol, F. Ruch, J. Schell, M. Bouquey, Interest of a Rheokinetic Study for the Development of Thermoplastic Composites by T-RTM, Univers. J. Mater. Sci. 5 (2017) 15–27. https://doi.org/10.13189/ujms.2017.050103.

[12] B. Dahlke, H. Larbig, H.D. Scherzer, R. Poltrock, Natural Fiber Reinforced Foams Based on Renewable Resources for Automotive Interior Applications, J. Cell. Plast. 34 (1998) 361–379. https://doi.org/10.1177/0021955X9803400406.

[13] J. George, M.S. Sreekala, S. Thomas, A review on interface modification and characterization of natural fiber reinforced plastic composites. Polymer Engineering & Science. 41 (2001) 1471–1485. https://doi.org/10.1002/pen.10846.

[14] N. Le Moigne, B. Otazaghine, S. Corn, H. Angellier-Coussy, A. Bergeret, Interfaces in Natural Fibre Reinforced Composites: Definitions and Roles, Springer International Publishing, Cham. (2018) 23–34. https://doi.org/10.1007/978-3-319-71410-3_2.

[15] S. Kalia, B.S. Kaith, I. Kaur, Pretreatments of natural fibers and their application as reinforcing material in polymer composites - A review, Polym. Eng. Sci. 49 (2009) 1253–1272. https://doi.org/10.1002/pen.21328.

[16] H.D. Rozman, K.W. Tan, R.N. Kumar, A. Abubakar, Z.A. Mohd. Ishak, H. Ismail, The effect of lignin as a compatibilizer on the physical properties of coconut fiber–polypropylene composites, Eur. Polym. J. 36 (2000) 1483–1494. https://doi.org/10.1016/S0014-3057(99)00200-1.

[17] M. Sain, P. Suhara, S. Law, A. Bouilloux, Interface Modification and Mechanical Properties of Natural Fiber-Polyolefin Composite Products, J. Reinf. Plast. Compos. 24 (2005) 121–130. https://doi.org/10.1177/0731684405041717.

[18] S. Rizal, Ikramullah, D.A. Gopakumar, S. Thalib, S. Huzni, H.P.S. Abdul Khalil, Interfacial Compatibility Evaluation on the Fiber Treatment in the Typha Fiber Reinforced Epoxy Composites and Their Effect on the Chemical and Mechanical Properties, Polymers. 10 (2018) 1316. https://doi.org/10.3390/polym10121316.

[19] S.R. Karmakar, Chemical Technology in the Pre-Treatment Processes of Textiles, Elsevier. 12 (1999).

[20] M. George, P.G. Mussone, D.C. Bressler, Improving the accessibility of hemp fibres using caustic to swell the macrostructure for enzymatic enhancement, Ind. Crops Prod. 67 (2015) 74–80. https://doi.org/10.1016/j.indcrop.2014.10.043.

[21] R. Narjès, M. Nardin, J.Y. Dréan, R. Frydrych, A study of the surface properties of cotton fibers by inverse gas chromatography, Journal of Colloid and Interface Science. 314 (2007) 373-380. https://doi.org/10.1016/j.jcis.2007.05.058.

[22] M.N. Belgacem, G. Czeremuszkin, S. Sapieha, A. Gandini, Surface characterization of cellulose fibres by XPS and inverse gas chromatography. Cellulose. 2 (1995) 145–157. https://doi.org/10.1007/bf00813015.

[23] R. Morent, N. De Geyter, J. Verschuren, K. De Clerck, P. Kiekens, S. Leys, Non-thermal plasma treatment of textiles, Surface & Coatings Technology. 202 (2008) 3427–3449. https://doi.org/10.1016/j.surfcoat.2007.12.027.

[24] A. Vesel, M. Mozetic, S. Strnad, Z. Peršin, K. Stana-Kleinschek, N. Hauptman, Plasma modification of viscose textile, Vacuum. 84 (2009) 79–82. https://doi.org/10.1016/j.vacuum.2009.04.028.

[25] S. Kalia, K. Thakur, A. Celli, M.A. Kiechel, C.L. Schauer, Surface modification of plant fibers using environment friendly methods for their application in polymer composites, textile industry and antimicrobial activities: A review, J. Environ. Chem. Eng. 1 (2013) 97–112. https://doi.org/10.1016/j.jece.2013.04.009.

[26] M/ Abdelmouleh, S. Boufi, A. ben Salah, M.N. Belgacem, A. Gandini, Interaction of Silane Coupling Agents with Cellulose, Langmuir. 18 (2002) 3203-3208. https://doi.org/10.1021/la011657g.

[27] A.K. Bledzki, J. Gassan, Composites reinforced with cellulose based fibres, Prog. Polym. Sci. 24 (1999) 221–274. https://doi.org/10.1016/S0079-6700(98)00018-5.

[28] M.C. Brochier Salon, M.N. Belgacem, Hydrolysis-Condensation Kinetics of Different Silane Coupling Agents, Phosphorus, Sulfur, and Silicon and the Related Elements. 186 (2011) 240-254. https://doi.org/10.1080/10426507.2010.494644.

[29] B.P. Revol, M. Thomassey, F. Ruch, M. Nardin, Influence of the sample number for the prediction of the tensile strength of high tenacity viscose fibres using a two parameters Weibull distribution, Cellulose. 23 (2016) 2701–2713. https://doi.org/10.1007/s10570-016-0974-2.

[30] W. Weibull, A statistical theory of strength of materials, IVB Handl. (1939).

[31] N. Rjiba, M. Nardin, J.Y. Drean, R. Frydrych, Comparison of surfaces properties of different types of cotton fibers by inverse gas chromatography, Journal of Polymer Research. 17 (2009) 25–32. https://doi.org/10.1007/s10965-009-9286-7.

[32] S.K. Ramamoorthy, M. Skrifvars, M. Rissanen, Effect of alkali and silane surface treatments on regenerated cellulose fibre type (Lyocell) intended for composites, Cellulose. 22 (2014) 637–654. https://doi.org/10.1007/s10570-014-0526-6.

[33] C. Roy, Étude de mélanges de cellulose dans des solutions aqueuses de soude, Paris Tech, 2010. https://pastel.archives-ouvertes.fr/tel-00274837.

[34] Z. Peršin, P. Stenius, K. Stana-Kleinschek, Estimation of the surface energy of chemically and oxygen plasma-treated regenerated cellulosic fabrics using various calculation models, Textile Research Journal. 81 (2011) 1673–1685. https://doi.org/10.1177/0040517511410110.

[35] R.M. France, R.D. Short, Plasma Treatment of Polymers: The Effects of Energy Transfer from an Argon Plasma on the Surface Chemistry of Polystyrene, and Polypropylene. A High-Energy Resolution X-ray Photoelectron Spectroscopy Study, Langmuir. 14 (1998) 4827–4835. https://doi.org/10.1021/la9713053.

[36] Z. Peršin, A. Vesel, K. Stana-Kleinschek, M. Mozetič, Characterization of surface properties of chemical and plasma treated regenerated cellulose fabric, Textile Research Journal. 82 (2012) 2078-2089. https://doi.org/10.1177/0040517512445338.

[37] Z.Q. Hua, R. Sitaru, F. Denes, R.A. Young, Mechanisms of oxygen- and argon-RF-plasma-induced surface chemistry of cellulose, Plasmas and Polymers. 2 (1997) 199–224. https://doi.org/10.1007/bf02766154.

[38] M. Vauthier, L. Jierry, F. Boulmedais, J.C. Oliveira, K.F.A. Clancy, C. Simet, V. Roucoules, F. Bally-Le Gall, Control of Interfacial Diels–Alder Reactivity by Tuning the Plasma Polymer Properties, Langmuir. 34 (2018) 11960–11970. https://doi.org/10.1021/acs.langmuir.8b02045.

[39] F. Tsang, Y.J. Su, V.N. Bliznetsov, Comparative studies of physical and chemical properties of plasma-treated CVD low k SiOCH dielectrics, Thin Solid Films. 462 (2004) 269-274. https://doi.org/10.1016/j.tsf.2004.05.055.

[40] E.M. Liston, L. Martinu, M.R. Wertheimer, Plasma surface modification of polymers for improved adhesion: a critical review, J. Adhes. Sci. Technol. 7 (1993) 1091–1127. https://doi.org/10.1163/156856193X00600.

[41] J. Ružbarský, A. Panda, Plasma Jet, Plasma Therm. Spray. (2017) 1–12. https://doi.org/10.1007/978-3-319-46273-8_1.

[42] J.E. Klemberg-Sapieha, L. Martinu, S. Sapieha, M.R. Wertheimer, Control and Modification of Surfaces and Interfaces by Corona and Low-Pressure Plasma, Interfacial Interact. Polym. Compos. (1993) 201–222. https://doi.org/10.1007/978-94-011-1642-8_10.

[43] M.-H. Berger, D. Jeulin, Statistical analysis of the failure stresses of ceramic fibres: Dependence of the Weibull parameters on the gauge length, diameter variation and fluctuation of defect density, J. Mater. Sci. 38 (2003) 2913–2923. https://doi.org/10.1023/A:1024405123420.

[44] J. Andersons, E. Poriķe, E. Spārniņš, Modeling strength scatter of elementary flax fibers: The effect of mechanical damage and geometrical characteristics, Compos. Part Appl. Sci. Manuf. 42 (2011) 543–549. https://doi.org/10.1016/j.compositesa.2011.01.013.

[45] M.-C. Brochier Salon, M. Abdelmouleh, S. Boufi, M.N. Belgacem, A. Gandini, Silane adsorption onto cellulose fibers: Hydrolysis and condensation reactions, J. Colloid Interface Sci. 289 (2005) 249–261. https://doi.org/10.1016/j.jcis.2005.03.070.

[46] N. Aissaoui, L. Bergaoui, J. Landoulsi, J.F. Lambert, S. Boujday, Silane Layers on Silicon Surfaces: Mechanism of Interaction, Stability, and Influence on Protein Adsorption, Langmuir. 28 (2012) 656-665. https://doi.org/10.1021/la2036778a.

[47] N. Majoul, S. Aouida, B. Bessaïs, Progress of porous silicon APTES-functionalization by FTIR investigations, Applied Surf. Sci. 331 (2015) 388-391. https://doi.org/10.1016/j.apsusc.2015.01.107.

[48] H. Yasuda, T. Yasuda, The competitive ablation and polymerization (CAP) principle and the plasma sensitivity of elements in plasma polymerization and treatment, J. Polym. Sci. Part Polym. Chem. 38 (2000) 943–953. https://doi.org/10.1002/(SICI)1099-0518(20000315)38:6<943::AID-POLA3>3.0.CO;2-3.

[49] F. Siffer, A. Ponche, P. Fioux, J. Schultz, V. Roucoules, A chemometric investigation of the effect of the process parameters during maleic anhydride pulsed plasma polymerization, Anal. Chim. Acta. 539 (2005) 289–299. https://doi.org/10.1016/j.aca.2005.02.072.

[50] D. Vollhardt, U. Retter, Nucleation in insoluble monolayers. 1. Nucleation and growth model for relaxation of metastable monolayers, J. Phys. Chem. 95 (1991) 3723-3727. https://doi.org/10.1021/j100162a052.

[51] D.K. Schwartz, Mechanisms and Kinetics of Self-Assembled Monolayer Formation, Annual Review of Physical Chemistry. 52 (2001) 107-137. https://doi.org/10.1146/annurev.physchem.52.1.107.

[52] E. Metwalli, D. Haines, O. Becker, S. Conzone, C.G. Pantano, Surface characterizations of mono-, di-, and tri-aminosilane treated glass substrates, Journal of Colloid and Interface Science. 298 (2006) 825-831. https://doi.org/10.1016/j.jcis.2006.03.045.

Figure Captions

Table 1. Experimental conditions used for the 4-factors, 2-levels design of experience.

Table 2. C1s XPS analyzes of high tenacity viscose filaments after various types of chemical cleaning treatments.

Table 3. C1s XPS analyzes of high tenacity viscose filaments after different plasma cleaning processes.

Table 4. C1s XPS analyzes of high tenacity viscose fabrics after oxygen plasma cleaning.

Figure 1. Diameter distribution for untreated (CRNT) and O_2-plasma treated (CRO2) filaments.

Figure 2. a) Rupture stresses of cellulose filaments treated with oxygen plasma (CRO2) and untreated cellulose filaments (CRNT) and b) representation of the breaking probability of CRO2 and CRNT according to a 2-parameters Weibull model.

Figure 3. a) Young's modulus and b) elongation at break for treated (CRO2) or untreated (CRNT) filament, with a gauge length of 34 mm.

Figure 4. FTIR-ATR spectra realized with Ge crystal of an untreated fabric (blue) or after various treatments (red: 10 W 1 min, 0.5% 2 h; green: 60W 1 min, 5% 30 min).

Figure 5. Relationship between the quantity of nitrogen groups determined by XPS and by FTIR-ATR. The experiments analyzed were 1, 11, 13 and 16 (see Table SI1) as well as the untreated fabric as a reference (no peak, zero intensity).

Table 5. Normalized infrared intensity values and conversion ratio after treatment.

Figure 6. Values of significant coefficients impacting the amount of nitrogen groups present at the surface of the fibers. A: plasma power; B: plasma treatment time; C: APTES concentration; D: APTES treatment time.

Figure 7. Values of significant coefficients impacting the conversion rate of polyamide-6 on treated fibers. A: plasma power; B: plasma treatment time; C: APTES concentration; D: APTES treatment time.

Table 6. Wide-spectrum XPS analysis of various cleaned and treated samples. *First line: plasma treatment, second line: APTES treatment. **Impurities (Zn, Cl) in a small amount (<0.5%).

Tables and Figures

Table 1

Factors	Codes	Variations		
		Level -	Level 0	Level +
Plasma power (W)	A	10	35	60
Plasma time (min)	B	1	3	5
APTES concentration (w%)	C	0.5	2.75	5
APTES time (min)	D	30	75	120

Table 2

Treatments	O/C ratio (%)	**C**-C (%)	**C**-O-C, **C**-OH (%)	O-**C**-O, **C**=O (%)	**C**-OOR (%)
Uncleaned	**53**	**14.7**	**73.3**	**11.3**	**0.7**
NaOH 8w%	59	15.5	71.8	12.7	0
NaOH 0.5w%	60	11.8	73.2	14.8	0.2
Na_2CO_3	61	15.6	73.5	10.6	0
EtOH 50°C	63	7.3	76.5	15.7	0.5
EtOH Soxhlet	68	4.9	83.4	11.7	0
Theory (cellulose)	**83**	**0**	**83**	**17**	**0**

Table 3

Treatments	O/C ratio (%)	**C**-C (%)	**C**-O-C, **C**-OH (%)	O-**C**-O, **C**=O (%)	**C**-OOR (%)
Uncleaned	**53**	**14.7**	**73.3**	**11.3**	**0.7**
Ar plasma 50 W, 5 min	70	17.0	53.9	17.6	11.4
O_2 plasma 50 W, 5 min	83	2.4	68.7	20.7	8.2
Theory (cellulose)	**83**	**0**	**83**	**17**	**0**

Table 4

Treatments	O/C ratio (%)	**C**-C (%)	**C**-O-C, **C**-OH (%)	O-**C**-O, **C**=O (%)	**C**-OOR (%)	Carbonate (%)
Uncleaned	**32**	**84.3**	**39.5**	**7.5**	**4.8**	**-**
10 W, 1 min	36	48.5	34.1	10.0	7.4	-
10 W, 5 min	70	14.7	58.5	17.5	9.3	-
60 W, 1 min	52	36.3	40	13.7	10.0	-
60 W, 5 min	70	15.1	55.9	18.5	7.9	2.6

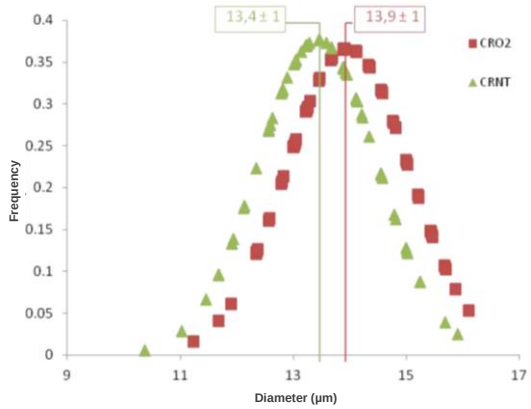

Figure 1

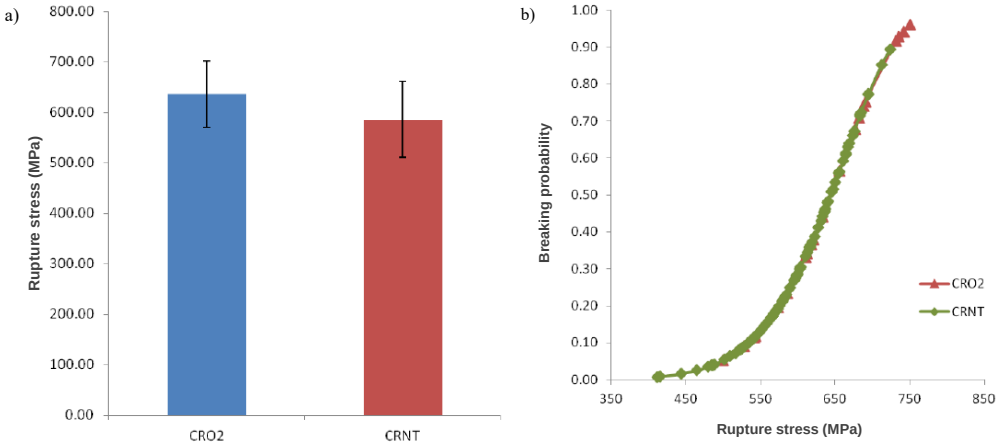

Figure 2

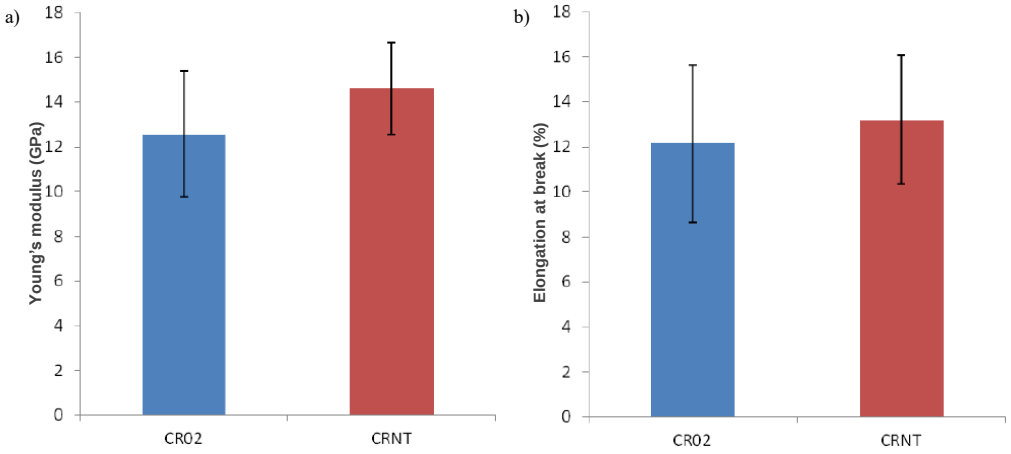

Figure 3

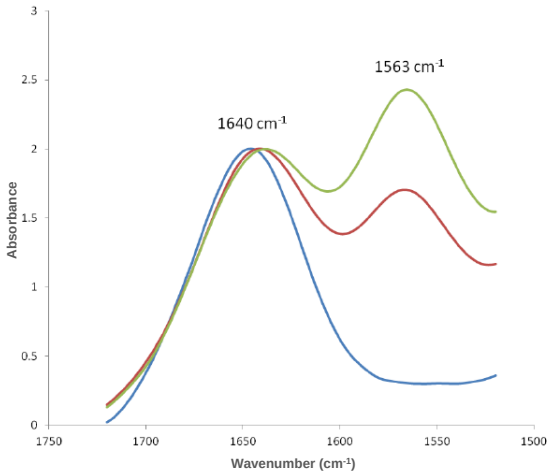

Figure 4

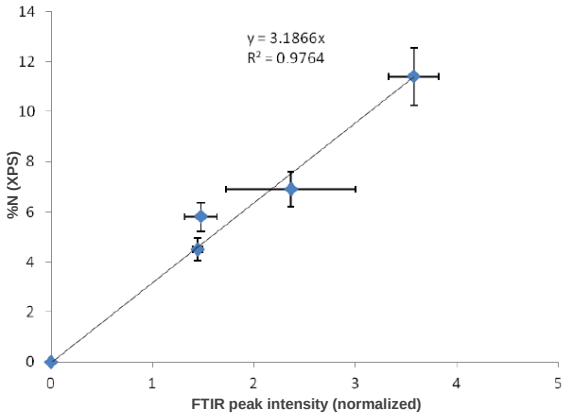

Figure 5

Table 5

i	Normalized IR intensity (a.u.)	Conversion rate (%)
1	2.5	64
2	1.9	70
3	2.6	73
Average	2.3	69
Scatter on the results	0.4	5

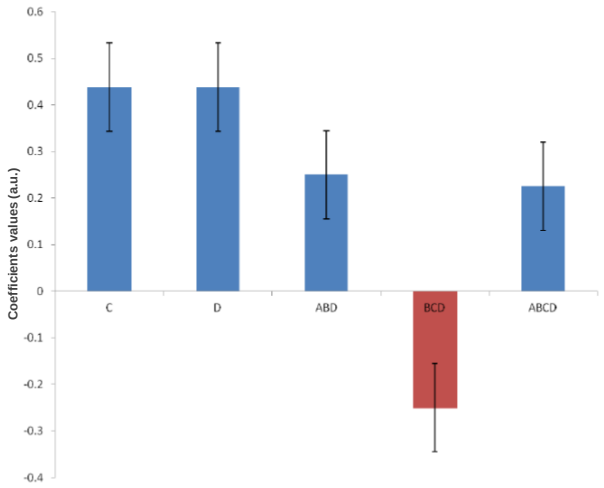

Figure 6

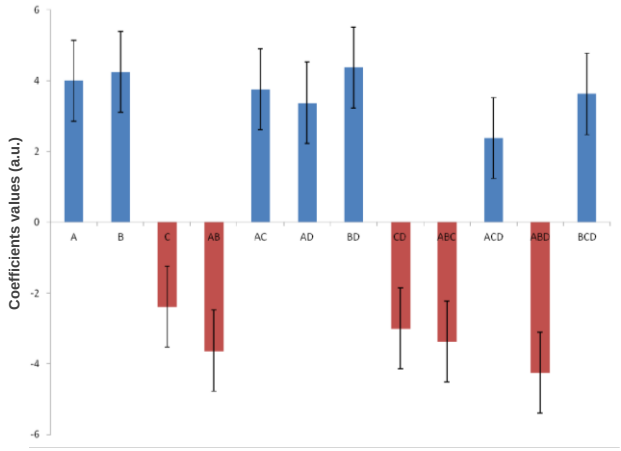

Figure 7

Table 6

N°	Treatments*	O/C (%)	%C	%O	%N	%Si	%F	%S	Amount of silane (a.u.)	Conversion rate (%)
-	**Untreated**	**32**	**75**	**24**	**-**	**0.4**	**-**	**-**	**-**	**61**
16	60 W 5 min 5w% 2 h	41	57	24	6.9	10.7	1.2	-	2.8	72
1**	10 W 1 min 0.5w% 30 min	46	60	28	4.5	5.8	0.6	0.6	1.5	65
13	10 W 1 min 5w% 2 h	42	52	22	11	13.9	-	-	4	16
11**	10 W 5 min 0.5w% 2 h	42	61	26	5.8	7.2	-	-	1.4	72